Preprint: SPIE Photonics West 2014; Paper# 8993-30; Presentation: Monday, Feb-3 @ 9:50AM

Spatial mode filtering of mid-infrared (mid-IR) laser beams with hollow core fiber optics

Jason M. Kriesel[*a], Gina M. Hagglund[a], Nahum Gat[a], Vincenzo Spagnolo[b], and Pietro Patimisco[b]
[a]Opto-Knowledge Systems, Inc. (OKSI), 19805 Hamilton Ave., Torrance CA, USA 90502-1341;
[b]Dipartimento Interateneo di Fisica, University and Politecnico of Bari, Italy.

ABSTRACT

Measurements characterizing spatial mode filtering of mid-infrared (mid-IR) laser beams using hollow core fiber optics are presented. The mode filtering depends strongly on the fiber diameter, with effective mode filtering demonstrated with bore diameters of d = 200 µm and 300 µm. In addition to mode filtering, beam profile measurements also demonstrate the strong dependence of the mode quality on the fiber coupling conditions. As predicted, optimal coupling is achieved using relatively slow optics that produce focused spots that nearly fill the fiber diameter. Examples of the utility of using hollow fibers for mode-filtering to improve molecular spectroscopy experiments are also discussed.

Keywords: mid-infrared, single-mode, fiber optic, waveguide, quantum cascade laser (QCL), interband cascade laser (ICL), CO_2 laser, molecular spectroscopy

1 INTRODUCTION

Mid-IR lasers operating in the wavelength range from λ = 3 µm to 14 µm, such as quantum cascade, interband cascade, and CO_2 lasers, are extremely useful for a range of applications including (but not limited to) molecular spectroscopy, remote sensing, IR counter measures, medicine, and industrial cutting. For many applications it is desirable to have a single spatial mode (i.e., Gaussian beam profile), which can enable such benefits as higher signal-to-noise, lower beam divergence, and diffraction limited performance. In prior studies, hollow core fibers (i.e., hollow waveguides) with bore sizes as large as 30 times the wavelength have been shown to provide a convenient, relatively low-loss means of delivering mid-IR beams with a single spatial mode [1]. The single mode behavior is essentially accomplished by the preferential damping of higher order modes, which is a property of hollow fibers that can also be utilized to effectively filter multi-mode laser beams, leading to improved performance of systems that utilize mid-IR lasers.

2 HOLLOW CORE FIBER OPTIC WAVEGUIDES

Figure 1 shows the basic structure of hollow fiber optics used in the studies presented here. Fabrication of the fibers is accomplished using a wet chemistry process developed by Harrington *et. al*. at Rutgers University, which consists of depositing a reflective silver (Ag) layer followed by a dielectric silver iodide (AgI) layer inside a hollow glass capillary tube [2]. Note: the glass tubing simply provides a smooth surface on which the coatings are applied and does not contribute to the light guiding properties of the fiber; in addition, a protective buffer on the outside of the capillary tube helps to shield the glass from damage, but also does not contribute to the optical properties.

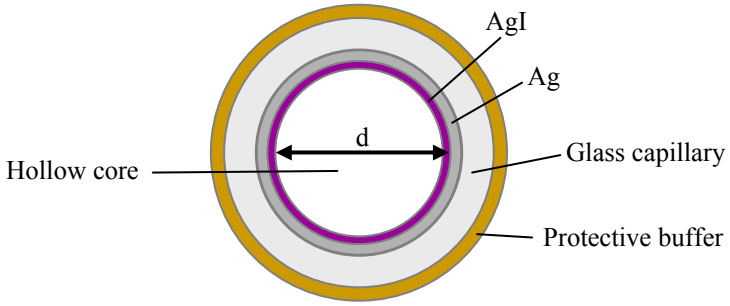

Figure 1. Cross section view of hollow fiber optic with internal diameter, d (layer thickness is not to scale).

[*] jason@oksi.com; phone: 310-756-0520; www.oksi.com

The spectral properties of the hollow fibers are determined by the thickness of the AgI dielectric layer, which is typically about 0.1 μm to 1.0 μm thick. Figure 2 shows representative spectra for hollow fibers with different AgI thickness; the peaks at the short wavelength end of the spectrum are interference peaks due to the thin AgI layer. By producing a hollow fiber with a specific dielectric thickness layer, the transmission spectrum of the waveguides can be tailored for different spectral wavelength ranges. The thinner coatings have better transmission at the low wavelength regime (e.g., λ ~ 3 to 5 μm), as well as a broadband response, whereas, the thicker coatings lead to improved transmission at the longer wavelength regime (e.g., λ ~ 8 to 12 μm).

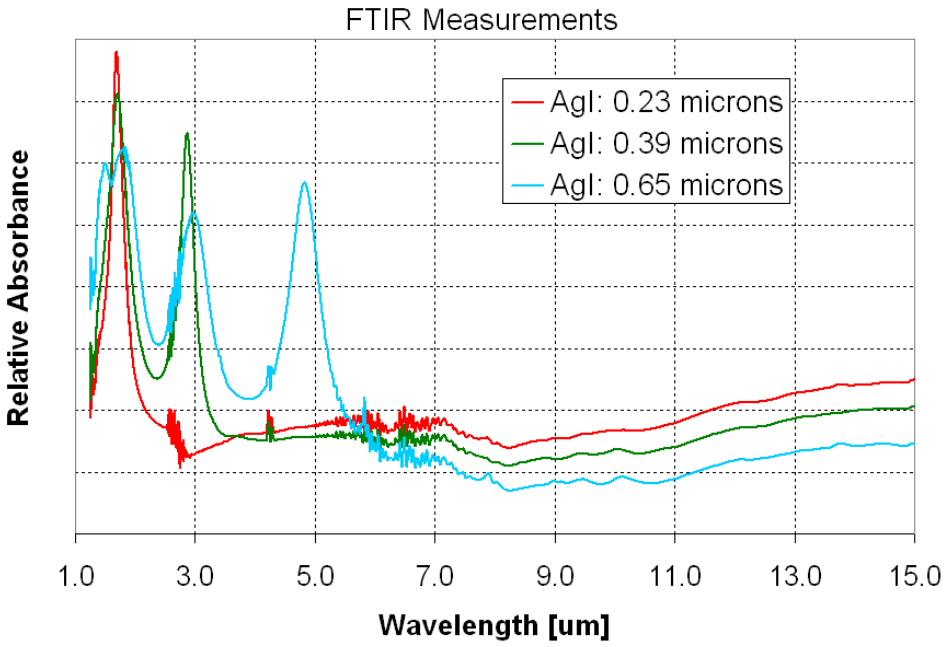

Figure 2. FTIR measurements of relative absorbance through hollow fiber samples that have different AgI dielectric layer thickness.

In addition to mid-IR applications, related hollow fiber structures can be optimized for the terahertz (THz), visible, and ultraviolet (UV) wavelength regimes. For terahertz, the fibers are made with a polystyrene dielectric layer instead of AgI [3]; the development of these fibers is relatively new, but have already shown moderate success in transmitting over the range from 2.5 to 5.0 THz [4]. Visible wavelength fibers are made without a dielectric layer (i.e., silver only) and the relatively large hollow core makes them useful for delivery of high peak power pulsed laser beams, such as from frequency double YAG lasers [5]. For UV wavelengths, the hollow fibers are made using an aluminum reflective layer instead of silver [6]; these fibers are useful for ArF excimer lasers and OPO based laser operating from 100 to 400 nm.

The theoretical waveguide loss has been described in detail elsewhere [2,7]. The fundamental modes are the HE_{nm} waveguide modes, where the HE_{11} mode is the lowest order mode, having a circularly-symmetric, Gaussian spatial profile. For our discussion, we consider that the theoretical length dependent loss (i.e., dB/m) for the HE_{nm} waveguide modes varies as

$$Waveguide\ Loss \propto \frac{u_{nm}^2 \lambda^2}{d^3}. \qquad (1)$$

Here u_{nm}, is the mth root of the zero-order Bessel function, λ is the wavelength, and d is the internal diameter of the hollow fiber. Putting aside the wavelength dependence, we first consider the dependence of loss on bore size and mode number. The $1/d^3$ dependence predicts a strong increase in loss as the fiber bore diameter is reduced, which quantitatively matches experimental measurements [2]. Typical values of loss range from ~ 4 dB/m for relatively small d = 200 μm fiber to < 0.1 dB/m for larger d = 1000 μm fibers. The u^2_{nm} dependence predicts higher damping for higher order modes, which has also been reported many times; however such mode dependence experiments have typically been limited to qualitative, rather than quantitative measurements.

To illustrate how waveguide theory predicts mode filtering, we provide numerical values in Table 1 for the transmission of the five lowest order waveguide modes in hollow fibers of different internal diameter. The values are calculated based on the loss value of a d = 300 μm fiber, which is taken to be 1 dB/m for the HE_{11} mode; this is a typical measured value for the d = 300 μm fibers made at OptoKnowledge®. Using Equation (1), we scale the loss for other fiber diameters and mode numbers. For example, the predicted loss for the HE_{11} mode for a d = 500 μm fiber is $(300/500)^3$ x 1 dB/m = 0.22 dB/m, which equates to a transmission factor = 0.95 for a one meter long fiber. We also calculate a value for the modal purity by considering the hypothetical case where the five lowest order modes are coupled into the fiber with equal amplitude, and then taking the ratio of the transmission of the HE_{11} mode to the sum of the transmission of all five modes. In other words, the modal purity value is a measure of the percentage of the output from the fiber that is in the lowest order mode. From the table it is evident that, theoretically, mode filtering is very strong for the smaller diameter fibers.

Table 1. Predicted transmission factor of the 5 lowest order waveguide modes for different hollow diameter fibers, along with the "Modal Purity" of a beam exiting the fiber (see description in text).

Mode	Transmission factor through hollow fiber (Length = 1m)		
	d = 200 μm	d = 300 μm	d = 500 μm
HE_{11}	0.46	0.79	0.95
HE_{12}	1.7E-2	0.30	0.77
HE_{13}	4.3E-5	5.1E-2	0.53
HE_{14}	7.7E-9	3.9E-3	0.30
HE_{15}	9.8E-14	1.4E-4	0.15
HE_{11} Modal Purity	**96%**	**69%**	**35%**

Now we return to the consideration of wavelength dependence. Equation (1) predicts that the loss for the hollow waveguides varies as λ^2; however, this wavelength dependence has not been observed in experiments, and instead the loss has been found to be relatively independent of wavelength. For example, Figure 2 shows the relatively flat spectral response typical of mid-IR hollow fibers for wavelengths longer than the interference bands. This flat spectral response has been explained by the counter-active effects of scattering due to surface roughness [8], which scales as

$$\text{Scattering attenuation} \sim 1/\lambda^2. \quad (2)$$

In other words, if we take the total loss to be due to the product of scattering attenuation and waveguide loss, then the wavelength dependence essentially cancels out. If this is the entire story, then there should be little wavelength dependence to the ability of a hollow fiber waveguide to mode filter; thus a d = 300 μm fiber should mode filter a λ = 5 μm beam, as well as a λ = 10 μm beam. However, empirically it has been observed that the fiber diameter needed for single-mode performance scales roughly as d < 30 λ. Recent measurements have argued for an extension of this rule of thumb to d < 50 λ [2]. However, the wavelength dependence is far from fully determined and more work is needed to provide a complete theoretical description.

In addition to mode damping, a related factor is mode coupling, which is described extremely well in Reference [7]. Essentially, coupling coefficients for the various modes is governed by the degree to which the focused beam "fills" the hollow bore. Optimal coupling into the lowest order HE_{11} mode occurs for

$$\text{Optimal coupling:} \quad 2w_o / d \sim 0.64, \quad (3)$$

where w_o is the $1/e^2$ point for a Gaussian beam ($I \propto e^{-2r^2/w_o^2}$). Considering a given fiber diameter and laser wavelength, optimal coupling is often described in terms of an effective numerical aperture (NA) or f-number (f/#). For example, for a fiber with a bore diameter of d = 300 μm, optimal coupling occurs for w_o = 96 μm, which for λ = 10 μm equates to NA = 0.03 or f/15. Thus, relatively slow optics provide optimal coupling into the lowest order mode. When faster optics are used (i.e., a smaller beam size, which under fills the fiber bore) there will be less coupling into the lowest order mode and more coupling into the higher order modes. On the opposite extreme, for the case where the beam size is bigger than the bore, the coupling efficiency will naturally go down due to clipping of the beam; however, the lowest order mode will be preferentially exited.

3 BEAM PROFILE MEASUREMENTS

Experimental setups used to demonstrate mode filtering are shown in Figure 3. The beam from a quantum cascade laser (QCL) was coupled into test fibers of various lengths, L. In each case, the alignment was optimized by maximizing the output power, and then the beam profile was imaged using a camera (Ophir-Spiricon® Pyrocam-III). For some experiments, a bent multi-mode hollow fiber (d = 500 µm) was utilized in between the QCL and the test fiber, as shown in Figure 3 (b); this was done simply to generate a multi-mode beam prior to focusing into the test fiber.

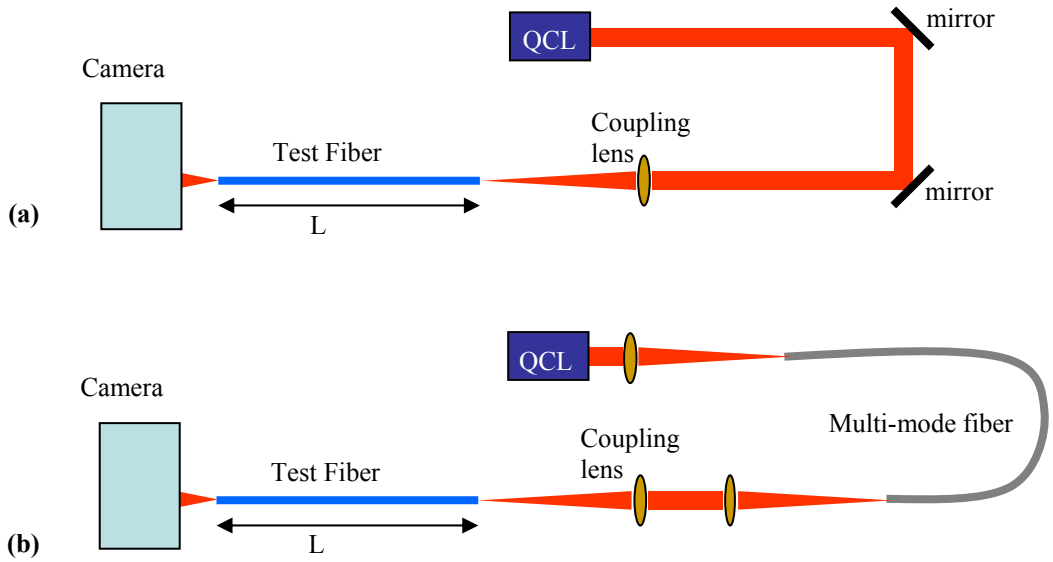

Figure 3. Diagram of experimental setup for beam profile measurements: (a) setup for direct measurement of laser output; and (b) setup using a multi-mode fiber prior to coupling into the test fiber.

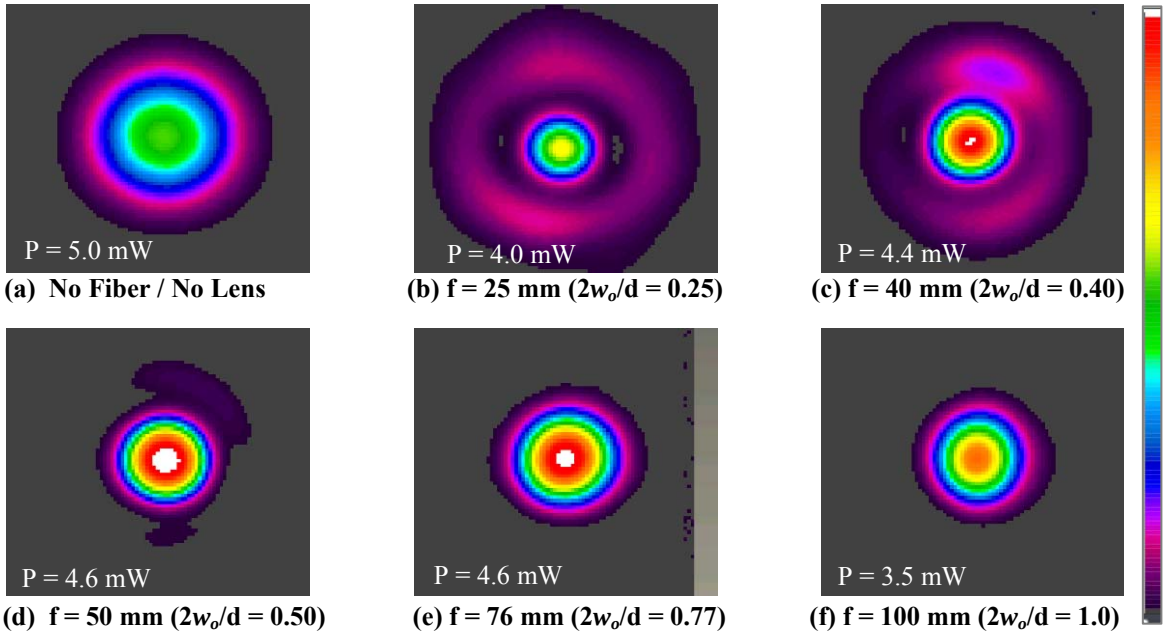

(a) No Fiber / No Lens **(b) f = 25 mm ($2w_o$/d = 0.25)** **(c) f = 40 mm ($2w_o$/d = 0.40)**

(d) f = 50 mm ($2w_o$/d = 0.50) **(e) f = 76 mm ($2w_o$/d = 0.77)** **(f) f = 100 mm ($2w_o$/d = 1.0)**

Figure 4. d = 300 µm, λ = 9.5 µm, L = 7 cm: (a) Two-dimensional beam profiles of a QCL operating at λ = 9.5 µm; and (b) - (f) images of the beam 3.75 cm after exiting a d = 300 µm, length = 7 cm hollow fiber. Different coupling lenses were used for the different images. The measured power, P, corresponding to each case is also displayed.

Before demonstrating mode-filtering, we present beam profile measurements designed to illustrate some of the general properties of coupling and loss discussed in the previous section. These measurements were taken using the setup shown in Figure 3 (a) with a Daylight Solutions tunable pulsed QCL set to a fixed wavelength of $\lambda = 9.5$ µm. The laser produced an average output power of about P = 5.0 mW and a beam diameter ~ 4 mm. The beam profile measured directly from this laser is shown in Figure 4 (a). In Figure 4 (b) – (f) measurements are shown of the beam profile after exiting a d = 300 µm test fiber with a relatively short length (L = 7 cm). By changing the focal length of the coupling lens (value listed in figure), the coupling conditions were changed from (b) under filling the fiber to (f) overfilling the fiber; the subsequent change in the mode quality of the initial beam coupled into the fiber is evident.

In Figure 5 and Figure 6 additional measurements are shown to demonstrate the difference in mode purity for two different diameter fibers, in this case an f = 76 mm lens was used for coupling into the fibers. The beam profile after the coupling lens, but without a fiber, is shown in Figure 5 (a) and again in Figure 6 (a). Beam profiles after exiting the test fibers are shown in the other images and vary from being nearly single-mode to highly multi-mode. In all cases, the beam power corresponding to the measured profile is also displayed. Figure 5 (b) and Figure 6 (b) show profiles after short pieces of fiber and demonstrate differences in coupling conditions for the two different diameter fibers. In the case of the d = 300 µm fiber, the focused beam overfills the fiber slightly ($2w_o/d = 0.77$) and thus the coupling is primarily in the lowest order mode. However, for the d = 500 µm fiber, the focused beam slightly under fills the fiber ($2w_o/d = 0.46$) with a coupling efficiency close to 100%, but with some of that power coupled into higher order modes.

Figure 5 (c) and (d), show that the d = 300 µm fiber is able to deliver single-mode output even when bent; however, the power output from the L = 100 cm fiber is down to about 80% of the value exiting the shorter 7 cm fiber. By comparison, Figure 6 (c) and (d) show that the larger, d = 500 µm, fiber delivers more power (e.g., about 90% of the incident power); however, the output is multi-mode, in particular becoming more multi-mode when bent.

(a) No Fiber **(b) L = 7 cm** **(c) L = 100 cm (straight)** **(d) L = 100 cm (bent)**

Figure 5. d = 300 µm, $\lambda = 9.5$ µm, $2w_o/d = 0.77$: Two-dimensional beam profile of a QCL operating at $\lambda = 9.5$ µm (a) measured 11.5 cm after an f = 76 mm focusing lens and (b) – (d) measured 3.75 cm after exiting d = 300 µm hollow fibers with two different lengths (bent and straight). The measured power in each case is also displayed.

(a) No Fiber **(b) L = 10 cm** **(c) L = 100 cm (straight)** **(d) L = 100 cm (bent)**

Figure 6. d = 500 µm; $\lambda = 9.5$ µm; $2w_o/d = 0.46$: Two-dimensional beam profile of a QCL operating at $\lambda = 9.5$ µm (a) measured 11.5 cm after an f = 76 mm focusing lens and (b) – (d) measured 3.75 cm after exiting d = 500 µm hollow fibers with two different lengths (bent and straight). The measured power in each case is also displayed.

To demonstrate mode filtering, we utilize the Daylight Solutions® laser with the setup in Figure 3 (b); this leads to a multi-mode beam as shown in Figure 7 (a). The beam diameter is ~ 3 mm prior to focusing with an f = 40 mm lens. The

beam exiting d = 300 μm fibers of different lengths are shown in Figure 7 (b) – (e). As predicted by Equation (1) and Table 1, the higher order modes are preferentially damped, and for longer fibers, the modal purity improves, i.e., the higher order modes are filtered out. Note that in this case, the transmission through the L = 200 cm fiber was actually greater than through the L = 100 cm fiber; this was simply because the L = 200 cm fiber used in the tests was fabricated with a thicker dielectric coating than the L = 100 cm fiber that was used. Thus the longer fiber was better optimized for the λ = 9.5 μm laser beam.

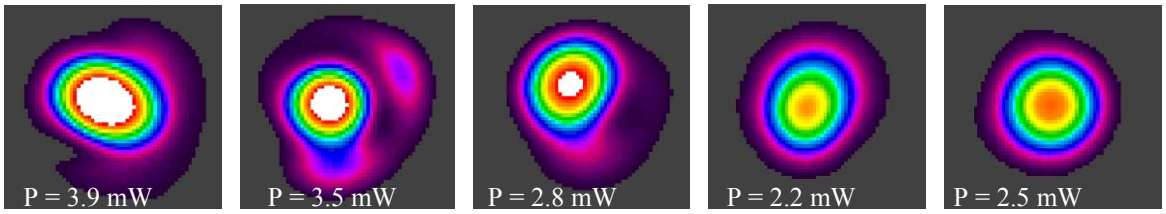

(a) No Fiber **(b) L = 7 cm** **(c) L = 50 cm** **(d) L = 100 cm** **(e) L = 200 cm**

Figure 7. d = 300 μm; λ = 9.5 μm; $2w_o/d \sim 0.5$: Two-dimensional beam profile of a QCL operating at λ = 9.5 μm (a) measured 7.5 cm after an f = 40 mm focusing lens and (b) – (e) measured 3.75 cm after exiting d = 300 μm hollow fibers of different lengths. The measured power in each case is also displayed.

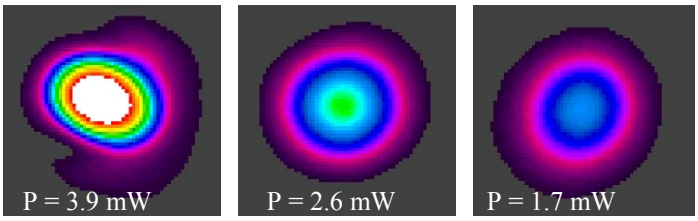

(a) No Fiber **(b) L = 7 cm** **(c) L = 50 cm**

Figure 8. d = 200 μm; λ = 9.5 μm; $2w_o/d \sim 0.8$: Two-dimensional beam profile of a QCL operating at λ = 9.5 μm (a) measured 7.5 cm after an f = 40 mm focusing lens and (b) – (c) measured 3.75 cm after exiting d = 200 μm hollow fibers of different lengths. The measured power in each case is also displayed.

Figure 8 shows measurements where the multi-mode beam was focused into d = 200 μm fibers. In this case, the focused spot overfills the fiber and the coupling is primarily into the lowest order mode; therefore, the mode filtering basically occurs when the beam is focused into the fiber, rather than along the length of the fiber.

To provide a second example of mode filtering we utilized an Alpes® laser operating at 5.3 μm. In this case, the setup was as shown in Figure 3 (a); however, the output was multi-mode due in part to non-ideal alignment of bench top collimating optics at the output of the laser chip (not shown in the setup diagram). The beam diameter was ~ 4.5 mm, and was focused with an f = 40 mm lens, and due to the relatively poor beam quality, the coupling efficiency was relatively low, ranging between 60% to 70%.

In this example, the d = 300 μm fibers do not effectively mode filter the beam, but the smaller d = 200 μm fiber do, as shown in Figure 9 and Figure 10. Note that in both cases, the coupling conditions under fill the fiber, and therefore the initial mode quality coupled into the fibers was highly multimode. Thus, due to differences in launch conditions between Figure 7 (λ = 9.5 μm) and Figure 9 (λ = 5.3 μm), it is not possible to make any conclusions regarding wavelength dependence on mode filtering, and further studies are needed to better address this question.

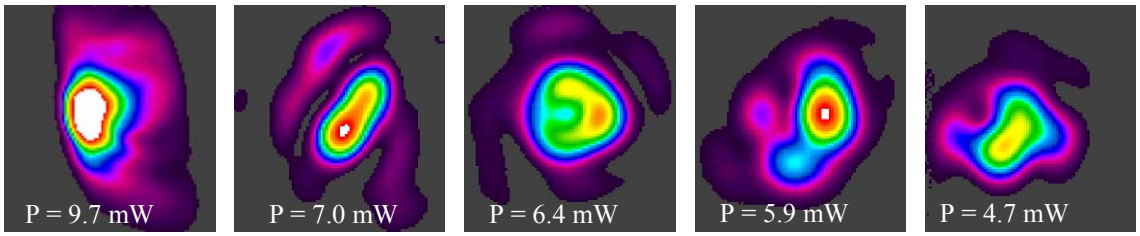

(a) No Fiber **(b) L = 7 cm** **(c) L = 50 cm** **(d) L = 100 cm** **(e) L = 200 cm**

Figure 9. d = 300 µm; λ = 5.3 µm; $2w_o/d \sim 0.2$: Two-dimensional beam profile of a QCL operating at λ = 5.3 µm (a) measured 7.5 cm after an f = 40 mm focusing lens and (b) – (e) measured 3.75 cm after exiting d = 300 µm hollow fibers of different lengths. The measured power in each case is also displayed.

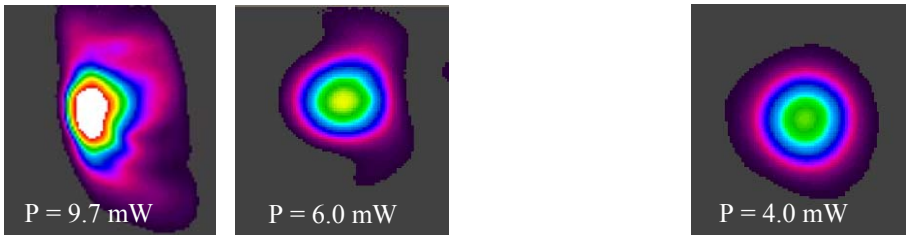

(a) No Fiber **(b) L = 7 cm** **(c) L = 100 cm**

Figure 10. d = 200 µm; λ = 5.3 µm; $2w_o/d \sim 0.3$: Two-dimensional beam profile of a QCL operating at λ = 5.3 µm (a) measured 7.5 cm after an f = 40 mm focusing lens and (b) – (c) measured 3.75 cm after exiting d = 200µm hollow fibers of different lengths. The measured power in each case is also displayed.

4 EXAMPLE USES FOR MOLECULAR SPECTROSCOPY

Hollow fibers cables provide a very effective and convenient means of delivering mid-IR laser beams. Two example configurations for beam delivery are shown in Figure 11, where (a) displays a setup designed specifically for attachment to a Daylight Solutions® QCL, and (b) shows a multi-fiber bundle designed to deliver four separate laser beams to single common output connector.

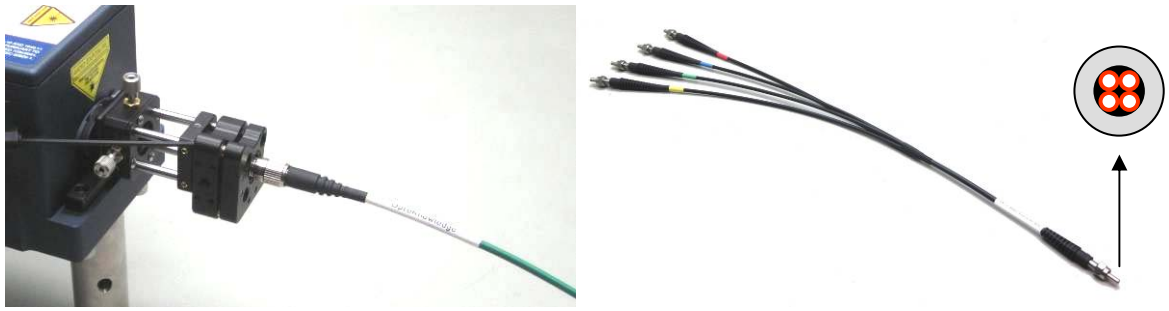

(a) Beam delivery for commercial lasers **(b) Multi-source beam delivery**

Figure 11. Pictures of hollow fiber cables used for beam delivery: (a) fiber delivery package that mounts directly to a Daylight Solutions laser; and (b) four-fiber-bundle for delivering multiple lasers with a common output.

The mode filtering capabilities demonstrated above are particularly appealing for use in molecular spectroscopy experiments. One example setup that has proven to benefit from the use of hollow fibers is shown in Figure 12. For these experiments, conducted at the University of Bari, an external cavity EC-QCL with fiber delivery was used within a quartz enhanced photoacoustic spectroscopy (QEPAS) setup. Detection results obtained with fiber delivery were compared to a setup using a pinhole as a spatial filter instead of the filter. Even though the hollow fiber attenuated the

beam and reduced the overall signal level slightly, the resulting signal to noise ratio (SNR) was 20% higher with the fiber, leading to a 20% better detection limit [9, 10]. This improvement in SNR was attributed to an improved spatial mode profile in the case of the fiber.

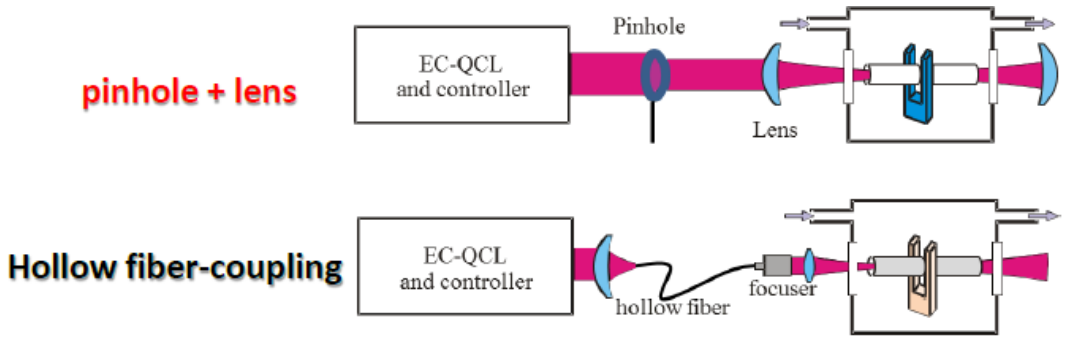

Figure 12. Diagram of test conducted to compare spectroscopy measurements with and without hollow fiber coupling. The measured QEPAS signal with the fiber was found to have a 20% higher SNR, leading directly to a 20% better detection limit.

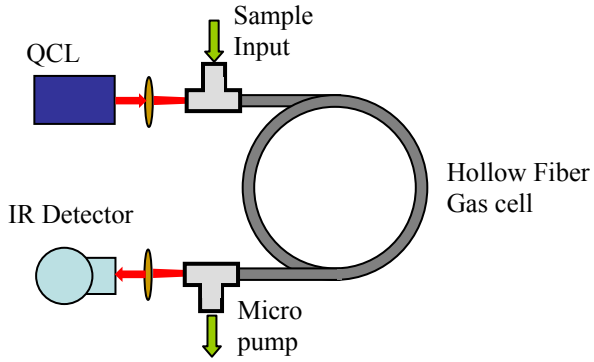

Figure 13. Simple diagram of PNNL's capillary absorption spectrometer (CAS).

In addition to using the hollow fibers to deliver mid-IR beams in molecular spectroscopy, the hollow fibers can alternatively be used as a gas cell, see Figure 13. For example, Dr. James Kelly at the Pacific Northwest National Laboratory (PNNL) has used his capillary absorption spectrometer (CAS) to conduct extremely sensitive measurements of CO_2 isotope ratio with ultra-small quantities of sample (< 1 mL) trapped in a hollow fiber gas cell [11]. Originally, a relatively large bore (d = 1000 μm) fiber was used, but by switching to a smaller diameter hollow fiber, the SNR is found to improve, presumably due to a reduction in modal noise. Furthermore, by using a tapered hollow fiber [12], feedback to the QCL is also greatly suppressed. More details can be found in a separate paper of these same proceedings [13].

5 DISCUSSION

Hollow fibers are able to effectively mode-filter mid-IR laser beams through preferential damping of higher order modes. For the studies shown here, a d = 300 μm fiber was utilized to effectively mode filter a λ = 9.5 μm laser beam, yet for a shorter wavelength λ = 5.3 μm beam, a smaller diameter, d = 200 μm, fiber was needed. However, as mentioned above, the coupling conditions for the λ = 5.3 μm laser were not ideal, and conclusions about the wavelength dependence on mode filtering can not be drawn. In general, mode filtering with hollow fibers is well understood through simple waveguide theory; however, understanding mode filtering as a function of laser wavelength requires additional investigation. Furthermore, we are continuing to work with tapered hollow fibers, and future studies will be investigating the mode filtering capabilities of these special fibers. Finally, the mode filtering capabilities of hollow

fibers are being investigated for the purpose of "cleaning up" the noise observed in various QCL sources, and we anticipate additional results that will further illustrate the utility of hollow fibers for improving mid-IR laser systems.

6 ACKNOWLEDGEMENTS

This work is based on research supported by the Department of Energy under Award Number DE-SC0001466. In addition, P. Patimisco and V. Spagnolo acknowledge financial support from three Italian research projects: PON01_02238, PON02_00675 and PON02_ 00576. We gratefully acknowledge Carlos Bledt at Brown University (formerly at Rutgers) and Prof. James Harrington at Rutgers University for extremely valuable discussions. We also express deep gratitude to Ophir-Spiricon® and Dan Ford for use of a Pyrocam-III camera, which enabled the beam profile measurements presented throughout this paper.

REFERENCES

[1] J.M. Kriesel, N. Gat, B.E. Bernacki, R.L. Erikson, B.D. Cannon, T.L. Myers, C.M. Bledt, and J.A. Harrington, "Hollow Core Fiber Optics for Mid-Wave and Long-Wave Infrared Spectroscopy," Proc. SPIE Vol 8018, DOI: 10.1117/12.882840 (2011).

[2] C. M. Bledt, J. A. Harrington, and J. M. Kriesel, "Loss and modal properties of Ag/AgI hollow glass waveguides," Appl. Opt. 51, 3114-3119 (2012).

[3] J.A. Harrington, J.E. Melzer, O. Mitrofanov, M. Navarro-Cia, "Silver-coated Teflon hollow waveguides for the delivery of terahertz radiation", SPIE Photonics West 2014, Paper# 8938-16.

[4] M. Navarro-Cía, M.S. Vitiello, C.M. Bledt, J.E. Melzer, J.A. Harrington, and O. Mitrofanov, "Terahertz wave transmission in flexible polystyrene-lined hollow metallic waveguides for the 2.5-5 THz band", Optics Express, Vol. 21, Issue 20, pp. 23748-23755 (2013) http://dx.doi.org/10.1364/OE.21.023748

[5] J.M. Kriesel, N. Gat, and D. Plemmons, "Fiber Optics for Remote Delivery of High Power Pulsed Laser Beams," Proceedings of the 48th AIAA Aerospace Sciences Meeting, Orlando, FL, January 2010,

[6] Y. Matsuura and M. Miyagi, "Hollow Optical Fibers for Ultraviolet and Vacuum Ultraviolet Light", IEEE Journal of Selected Topics In Quantum Electronics, Vol. 10, 1430 (2004).

[7] R. Nubling and J.A. Harrington, "Launch conditions and mode coupling in hollow glass waveguides", Opt. Eng. 37(9) 2454–2458 (1998).

[8] J.A. Harrington, Infrared Fibers and Their Applications, SPIE Press, Bellingham, WA (2004), pg 169.

[9] V. Spagnolo, P. Patimisco, S. Borri, G. Scamarcio, B.E. Bernacki, and J. Kriesel, "Mid-infrared fiber-coupled QCL-QEPAS sensor," Applied Physics B 112, 25 (2013)..

[10] V. Spagnolo, P. Patimisco, S. Borri, G. Scamarcio, B. E. Bernacki, and J. Kriesel, "Part-per-trillion level SF6 detection using a quartz enhanced photoacoustic spectroscopy-based sensor with single-mode fiber-coupled quantum cascade laser excitation," Optics Letters, 37, 4461 (2012).

[11] J.F.Kelly, R.L.Sams, T.A.Blake, M.Newburn, J.Moran, M.L.Alexander, and H.Kreuzer, "A capillary absorption spectrometer for stable carbon isotope (13C/12C) analysis in very small samples," Rev. Sci. Inst. 83, 023101 (2012).

[12] C. M. Bledt, D. V. Kopp, J. A. Harrington, S. Kino, Y. Matsuura and J. M. Kriesel, "Investigation of tapered silver / silver halide coated hollow glass waveguides for the transmission of CO2 laser radiation", Proc. SPIE Vol. 8218, DOI: 10.1117/12.912201 (2012).

[13] J.F. Kelly, R.L. Sams, T.A. Blake, J.M. Kriesel, "Further developments of capillary absorption spectrometers using small hollow-waveguide fibers", SPIE Photonics West 2014, Paper# 8993-60.